



ELSEVIER

International Journal of Pharmaceutics 205 (2000) 79–91

international  
journal of  
pharmaceutics

[www.elsevier.com/locate/ijpharm](http://www.elsevier.com/locate/ijpharm)

# Application of acoustic emission to the monitoring and end point determination of a high shear granulation process

Mark Whitaker <sup>a,\*</sup>, Guy R. Baker <sup>a</sup>, Julian Westrup <sup>a</sup>, Paul A. Goulding <sup>a</sup>,  
David R. Rudd <sup>a</sup>, Ron M. Belchamber <sup>b</sup>, Michael P. Collins <sup>b</sup>

<sup>a</sup> Pharmaceutical Development, Glaxo Wellcome Research and Development, Park Road, Ware, Hertfordshire, SG12 0DP, UK

<sup>b</sup> Process Analysis and Automation Ltd, Falcon House, Fernhill Road, Farnborough, Hampshire, GU14 9RX, UK

Received 23 August 1999; received in revised form 7 June 2000; accepted 11 June 2000

## Abstract

The application of a novel monitoring technique, based on the use of acoustic emissions, is reported for a model high shear granulation process. It has been demonstrated that this technique is capable of monitoring changes in physical properties of powder material during granulation (particle size, flow properties and compression properties). The technique is non-invasive, sensitive and relatively inexpensive. © 2000 Elsevier Science B.V. All rights reserved.

**Keywords:** High shear granulation; Acoustic emission; Process monitoring

## 1. Introduction

While much of analytical chemistry is concerned with the study of optical spectroscopy, the equivalent use of sound is often over-looked. Just as electromagnetic radiation may be emitted by physical and chemical processes, so too may sound energy and, therefore, there are parallels between the study of optics and acoustics.

The study of sound can be divided in to two main areas, active acoustics and passive acoustics (acoustic emission). In active acoustics, an acoustic wave is launched into the sample (material) of

interest. The physical properties of the sample govern the velocity and attenuation of this acoustic wave. The velocity is a function of the density and compressibility of the material. The attenuation is related to these and to additional viscoelastic and thermal properties.

Acoustic emission monitoring refers to the technique of detecting and analysing sound produced by a process or system. Often these sounds are well above the frequencies that can be detected by the human ear (frequencies up to ~15 kHz are audible). Processes that give rise to acoustic emission include boiling, gas evolution, mixing, grinding and fluidisation. Acoustic emissions produced by chemical reactions can reach frequencies of 1 MHz or greater (Wentzell and Wade, 1989). Such emissions are usually monitored using piezoelec-

\* Corresponding author. Fax: +44-1920-883-540.

E-mail address: [mw2541@glaxowellcome.co.uk](mailto:mw2541@glaxowellcome.co.uk) (M. Whitaker).

tric transducers that respond in the region 50–450 kHz. At these frequencies, attenuation is high and sound propagates only relatively short distances. This has the advantage that processes can be monitored with little interference from extraneous noise.

Acoustic emissions can propagate by a number of modes. In solids, compressional and shear or transverse modes are important. Compressional modes have the highest velocity and thus reach the transducer first. However, in most process applications of acoustic emission, there are many sources, each producing short bursts of energy and consequently the different modes cannot be resolved. The detected signal, for instance on the wall of a vessel, is a complex mixture of many overlapping waveforms resulting from many sources and many propagation modes.

At interfaces, depending on the relative acoustic impedance of the two materials, much of the energy is reflected back towards the source. In a fluidised bed, for instance, acoustic emissions will only be detected from particles directly impacting on the walls of the bed close to the transducer.

Acoustic emission is well-known in the study of fracture mechanics and is, therefore, extensively used by material scientists. It is also widely used as a non-destructive testing technique. A large amount of research has been conducted on the use of acoustic emission for the routine inspection of aircraft wings, pressure vessels, load-bearing structures and components. Acoustic emission is also used in the engineering industry for the monitoring of machine tool wear.

A convenient method of studying acoustic emission from processes is to use the 'average signal level'. An rms-to-dc converter is used to convert the amplitude-modulated carrier into a more slowly varying 'dc' signal. This is referred to as the average signal level (ASL) in this paper. This more slowly varying signal can then be digitally sampled at a low speed (say 50 Hz) and stored on a computer for further manipulations.

The simplest way of studying the acoustic data is to examine changes in the ASL. However, other information can be derived from examining the power spectrum of the ASL. The power spectrum is calculated by performing a fast Fourier trans-

form (FFT) on the digitised raw data record. Power spectra may be averaged to produce a reliable estimate of power spectral density or to give a 'fingerprint' of a particular process regime. This type of averaging is not possible on the raw acoustic signals or ASL records as they are essentially random and average to zero. Interpretation of the power spectrum is complicated by the fact that the acoustic signal originating in the system is distorted by several factors, including transmission, reflection and signal transfer characteristics.

The shape of the power spectrum of the ASL record is a function of the process dynamics. Periodic processes show high power at certain discrete frequencies (e.g. mechanical stirring, periodic bubbling of a fluidised bed). Random processes show either flicker type properties, where power is inversely proportional to frequency, or white noise type properties in which power is independent of frequency (van der Ziel, 1976). The amplitude of the power spectrum is also affected by the energy of the acoustic emissions produced by the process. For instance, if hard material is being processed, the acoustic emission produced by particle impact will be greater than that produced by soft material.

Several workers (Betteridge et al., 1981; Belchamber et al., 1986; Wentzell and Wade, 1989) have reported the use of acoustic emission in the study of chemical reactions. These range from the acoustic emission produced by effervescent reactions to crystalline phase changes. It has also been shown that acoustic emission is capable of monitoring the blending of powder materials (Tily et al., 1987; Holroyd, 1989) and for chemical systems that are difficult to observe by other means (Belchamber et al., 1986).

In this paper the application of acoustic emission to the on-line determination of the particle size, flow properties and compression properties of a model high shear granulation process is reported. This is based on the fact that particle size changes achieved during granulation will affect powder flow and compression properties. As particle size and granule density (both of which will influence the compression properties) will affect the acoustic emission signals, this monitoring technique is likely to prove useful in assessing changes in the relevant physical properties.

In this work, particle size, powder flow and powder compression properties are investigated, with the intention of relating the acoustic emission signals (produced during granulation) to the final properties of the resultant powder blend for tablet compression. Clearly the manufacturing processes which occur between the granulation stage and tablet compression (typically sieving, granule drying and lubricant mixing) will impact on the final powder blend properties. Thus, particle size and powder flow properties are measured at various stages during the manufacturing process, whereas the compression properties, which are strictly only pharmaceutically relevant at the final blend stage, are measured on this material alone.

## 2. Materials, methods and equipment

### 2.1. Materials

The formulation employed in this study is a simple placebo mix consisting of 91.7% w/w lactose monohydrate (Lactochem Pharmaceutical Lactose, Borculo Whey Products, Chester, UK) and 8.33% w/w microcrystalline cellulose (Avicel PH101, FMC International, Cork, Ireland). This powder mix was granulated with varying amounts of a 5% w/w aqueous solution of polyvinylpyrrolidone (PVP, ISP (GB), Manchester, UK) to produce nine granule batches with a range of physical properties. The granules were lubricated with 1% w/w magnesium stearate (Harochem, Burnley, UK) for the purpose of tabletting.

### 2.2. Equipment

#### 2.2.1. Granulation

Granulation was performed in a Fielder Pharmamatrix PMA10 high shear mixer granulator (Aeromatic-Fielder, Eastleigh, UK) at a 3-kg dry powder mix scale. The wet granules were dried in a Glatt GPCG 3/5 fluid bed granulator/drier (Glatt Protech, Leicester, UK). Granule screening pre- and post-drying was conducted using a Jackson Crockatt granulator (Jackson Crockatt, Glasgow, UK).

#### 2.2.2. Tableting

Lubrication of dried screened granules was conducted in an 18-l Y-cone blender attached to an Apex Multiplex drive unit. The blend was subsequently compressed using 8-mm round normal concave, plain faced tooling on a Manesty B-Unipress (27 stations) (BWI Manesty, Liverpool, UK).

#### 2.2.3. On-line acoustic monitoring

Acoustic data were collected using three piezoelectric acoustic emission sensors (Physical Acoustics, Cambridge, UK) covering frequencies from 20 to 350 kHz, with main resonances at 30, 70 and 150 kHz. These were attached to the outside of the high shear mixer bowl using silicone sealant as the coupling agent and were maintained in the same positions for all experiments. The following sensors were used for all experiments:

Identity (resonance frequency), kHz	Signal filtering
30	20-kHz high pass filter
70	40-kHz high pass filter
150	100–350-kHz band pass

Data were collected using an acoustic emission monitoring system (Osprey AE-8, Process Analysis and Automation, Farnborough, UK). This consisted of pre-amplifiers supplying 40-dB gain and signal filtering, rms-to-dc converters, variable gain amplifiers and a plug-in data acquisition board (PC-PM16, National Instruments, Newbury, UK). A schematic diagram showing the location of the acoustic sensors on the granulation bowl is presented in Fig. 1. Controlling software was written in a graphical programming language (LabVIEW 4.01, National Instruments, Newbury, UK).

#### 2.3. Granulation process

The lactose and microcrystalline cellulose were added to the Fielder Pharmamatrix and dry

blended for 2 min using an impellor speed of 200 rpm. The required quantity of granulating fluid (5% w/w PVP solution) was then added over a 1-min time period via the liquid entry port to the Fielder. An impellor speed of 200 rpm and a chopper speed of 1 were used throughout liquid addition, and these conditions were maintained over a further 2-min wet massing period. Granule growth was varied between batches by adjusting the quantity of granulating fluid from 150 to 650 ml. Visual inspection of the wet granules indicated that batches ranged from under-granulated through to over-granulated material. The wet mass was discharged from the granulator and passed through an 8-mesh screen on the Jackson Crockatt to remove any large agglomerates. The granules were then dried to a moisture content of <2% w/w in the Glatt GPCG 3/5 fluid bed drier using a drying air temperature of 70°C. Granule moisture contents were determined by loss on drying using an infra-red moisture balance. The dried granules were passed through an 18-mesh screen on the Jackson Crockatt to break down any agglomerates and then blended for 5 min with 1% w/w magnesium stearate in the Y-cone blender using a blender speed of 16 rpm. The lubricated granules were then tabletted on the Manesty Unipress using 8-mm round, normal concave, B type tooling. Tablets were prepared at a range of compression forces.

Although no data on yield were collected during the study, the small batch size allowed confirmation at each stage (by visual examination) that the vast majority of the granulated material had

progressed through the process. Thus, the majority of the material was tested by the reference techniques irrespective of the extent of granulation.

#### 2.4. Reference analysis

Granule batches were evaluated for particle size and flow (pre- and post- dry granule screening) and compression properties.

##### 2.4.1. Particle size

The particle size of each granule was determined by sieve analysis using an Endecott Octagon vibratory sieve shaker with a stack of eight sieves ranging from 45 µm to 1.0 mm. The median particle size and 25 and 75 percentile sizes were estimated from plots of cumulative percent undersize against sieve aperture size.

##### 2.4.2. Flow properties

Granule flow properties were evaluated by measuring the Carr's compressibility index. The Carr's compressibility index was calculated from the loose and tapped bulk densities ( $\rho_l$  and  $\rho_t$ ) of the granules using the following equation (Aulton, 1988);

$$\text{Carr's compressibility index (\%)} = \frac{\rho_t - \rho_l}{\rho_t} \times 100$$

Tapped bulk densities were measured following 1000 taps in a VanKel automated bulk density apparatus (ChemLab Scientific Products, Hornchurch, UK). Carr's compressibility indices of less than 20% are generally associated with good flow properties.

##### 2.4.3. Compression properties

Compression properties were evaluated in terms of the maximum crushing strength achieved before reaching the limit of compressibility (i.e. before the occurrence of capping). The forces were measured by means of pressure transducers attached to the compression roll mechanism of the Manesty Unipress and recorded via a Manesty Compaction Force Controller (CFC) unit (BWI

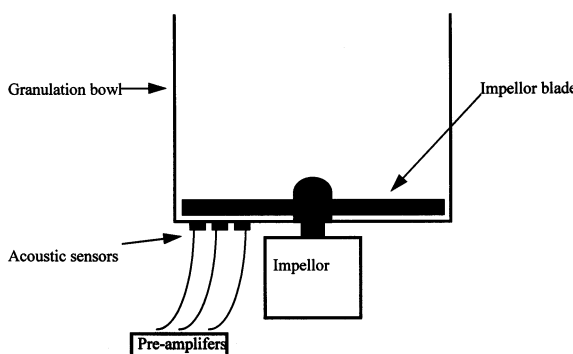


Fig. 1. Location of acoustic sensors.

Table 1  
Particle size data for granule before and after dry screening

Volume of binder solution (ml)	Mass mean median particle size (μm)	
	Material screened through a 2360-μm Jackson Crockatt screen	Material screened through a 925-μm Jackson Crockatt screen
150	111.3	118.5
250	151.0	92.5
300	147.8	125.5
350	170.3	127.0
400	174.0	119.0
450	206.5	147.0
550	474.0	177.5
650	1491.5	239.0
650	1140.8	237.5

Table 2  
Carr's compressibility index of granule at different stages throughout the manufacturing process and compression properties

Volume of PVP (ml)	Carr's compressibility index (% compressibility)			Compression properties, maximum crushing strength (kg)
	2360 μm	925 μm	925 μm, lubricated	
150	29.8	31.9	23.0	8.50
250	24.0	22.6	19.0	8.90
300	21.3	21.9	16.4	8.43
350	20.1	22.9	17.0	10.68
400	21.2	20.3	16.8	10.60
450	18.4	20.8	16.8	10.00
550	19.6	22.7	17.5	11.04
650	13.9	21.6	17.6	11.84
650	12.7	23.6	15.9	11.28

Manesty, Liverpool, UK). Tablet crushing strengths were measured using a Holland C40 hardness tester (I Holland, Long Eaton, UK).

### 2.5. Acoustic data collection

Raw data from the acoustic sensors were logged and converted into average signal level (ASL) data. Also the time-domain raw data were converted by a fast Fourier transform (FFT) into frequency-domain data (spectra). Raw data, ASL and spectra were collected throughout each of nine granule batches.

## 3. Results

### 3.1. Physical reference data

Particle size data for each batch of granules, both before and after dry screening (2360- and 925-μm screens, respectively), are presented in Table 1.

Data for the flow properties (Carr's compressibility index) of the granule at various stages throughout the manufacturing process are presented in Table 2. Also presented in Table 2 is data for the compression properties of the granule after lubrication with magnesium stearate.

### 3.2. Acoustic raw data

Evaluation of the raw acoustic data acquired is not discussed in this paper. However, analysis of ASL and spectral data suggests that alternative signal processing and filtering of the raw data prior to transformation may be beneficial (e.g. use of wavelet transforms or smoothing algorithms).

Graphical plots of the change of ASL throughout each batch are presented in Figs. 2–4 for the 30-, 70- and 150-kHz sensors respectively.

## 4. Discussion

### 4.1. Average signal level (ASL)

The ASLs for the three sensors, throughout each granulation batch, are shown in Figs. 2–4 for the 30-, 70- and 150-kHz sensors respectively. The 30- and 70-kHz sensors were found to have very similar profiles. The similarity of the 30- and 70-kHz plots is not surprising considering the similarity in signal filtering used for these two

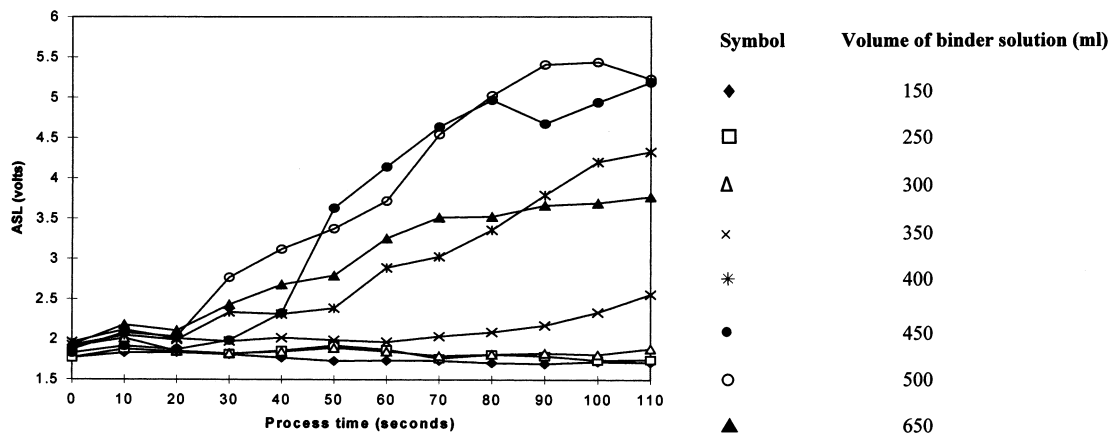


Fig. 2. Average signal levels (ASL) for 30-kHz sensor for various volumes of binder solution.

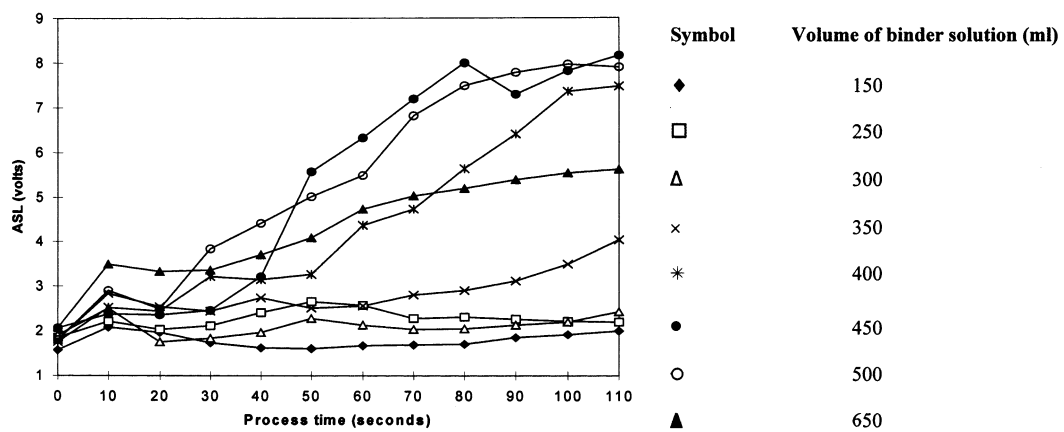


Fig. 3. Average signal levels (ASL) for 70-kHz sensor for various volumes of binder solution.

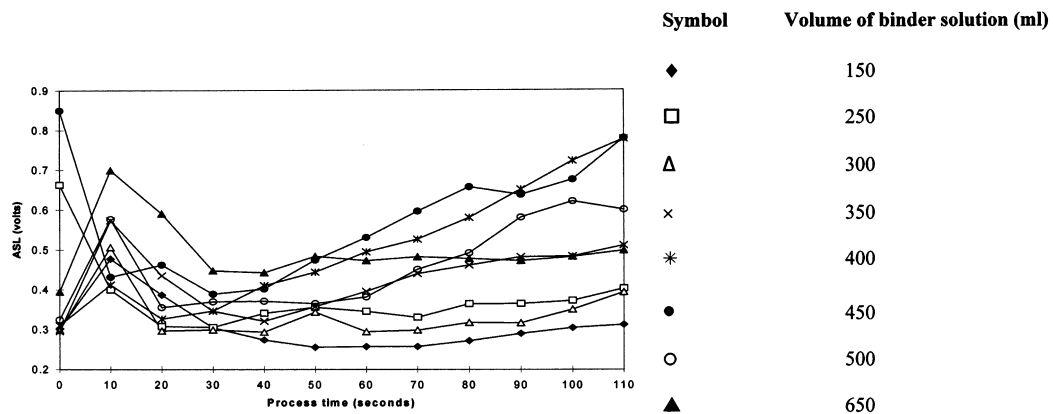


Fig. 4. Average signal levels (ASL) for 150-kHz sensor for various volumes of binder solution.

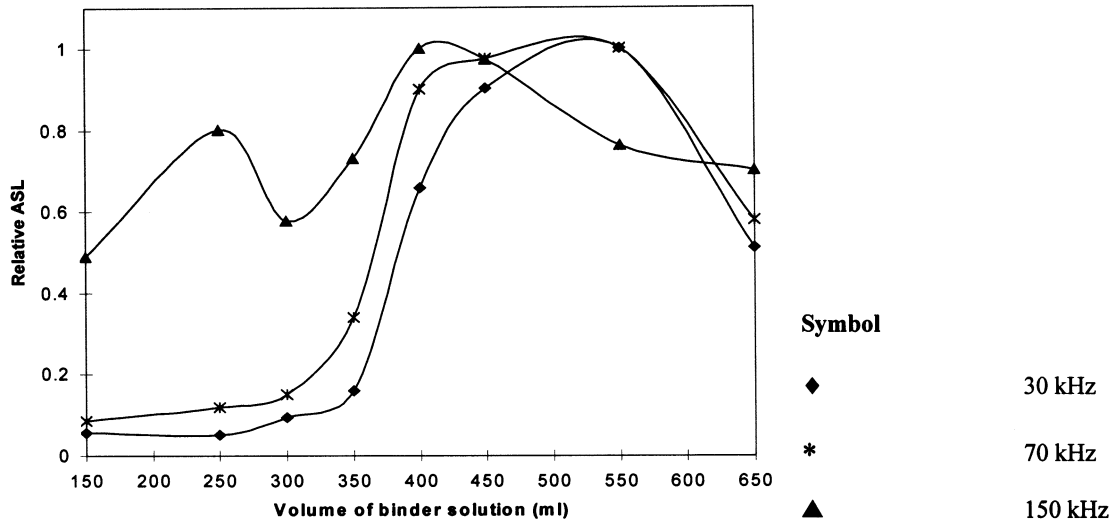


Fig. 5. Relative average signal level (ASL) difference for the 30-, 70- and 150-kHz sensors for various volumes of binder solution.

sensors. For both the 30- and 70-kHz sensors, batches containing greater than 300 ml of binder solution show a rise in ASL throughout the granulation process. The slope of this rise increases with increasing amounts of binder solution added, up to a maximum of 550 ml. The largest change in slope from batch to batch is in the region of 350–550 ml binder solution.

The profile of the 150-kHz sensor is slightly different, since there is an initial drop in ASL, followed by a gradual rise to the end of the process. However, there is less discrimination between each of the batches for the 150-kHz sensor

when compared with either the 30- or 70-kHz sensors.

The effect of binder solution volume on ASL is further illustrated in Fig. 5, where the difference in ASL between the beginning and end of each batch (normalised relative to the maximum ASL) is plotted against the amount of binder solution added. Fig. 5 shows similar profiles for the 30- and 70-kHz sensors, but a different profile for the 150-kHz sensor. For both the 30- and 70-kHz sensors, there is a large increase in the relative ASL from the 350-ml binder solution batch upwards. The change in ASL is reasonably consis-

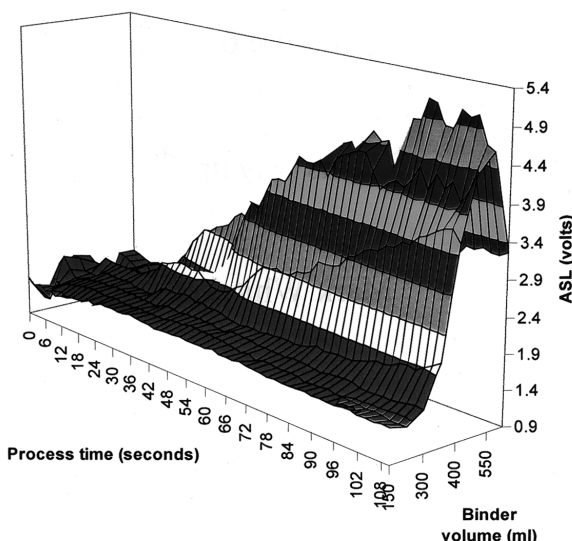


Fig. 6. Change of ASL for 70-kHz sensor for volume of binder solution versus processing time:  $\blacklozenge$ , 30 kHz;  $*$ , 70 kHz;  $\blacktriangle$ , 150 kHz.

tent with the observed change in physical properties of the resulting granule (in particular Carr's compressibility index).

Therefore, the ASL increases with both amount of binder solution added and processing time. A peak is reached with 550 ml binder solution after 110-s granulation, as shown in Fig. 6. A smaller ASL increase occurs with the batches containing 650 ml binder solution. Visual examination of

these batches at the end of granulation revealed these to be over-wet, with a significant amount of material adhering to the top of the bowl. From the particle size data it would be expected that the 650-ml batches should have a greater increase in ASL compared to all the other batches. Therefore, it is highly likely that the ASL is dependent, not only on the extent of granulation, but also the effective mass of product in the granulation bowl. It should be possible, therefore, to use the ASL as a measure of the extent of granulation of a material.

To assess the reproducibility of the measurement technique a series of batches were manufactured under identical process conditions. During an 8-month period, a series of three batches, each with 350 ml of added binder solution, were manufactured, the last two batches being made on consecutive days. Fig. 7 presents the ASL signal for the 30-kHz sensor for these three batches. It is clear from the ASL data that the technique is quite reproducible, particularly in terms of the short-term repeatability, where it can be seen that very good agreement was obtained for the two batches made on consecutive days.

#### 4.2. Acoustic spectral data

Analysis of the spectral data for all three sensors shows that most of the power is present at low signal frequencies less than 1.5 Hz. This is

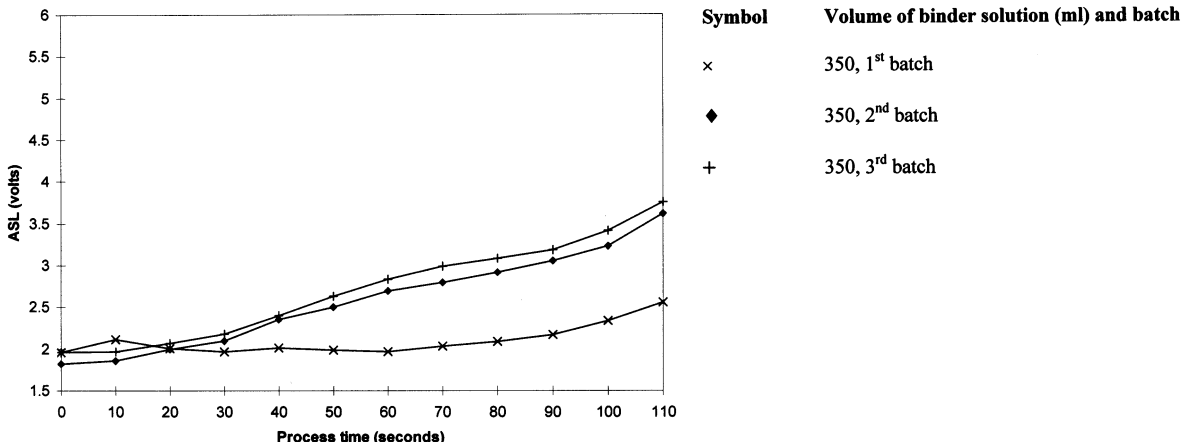


Fig. 7. Reproducibility of average signal level (ASL) for 30-kHz sensor for 350 ml of binder solution.

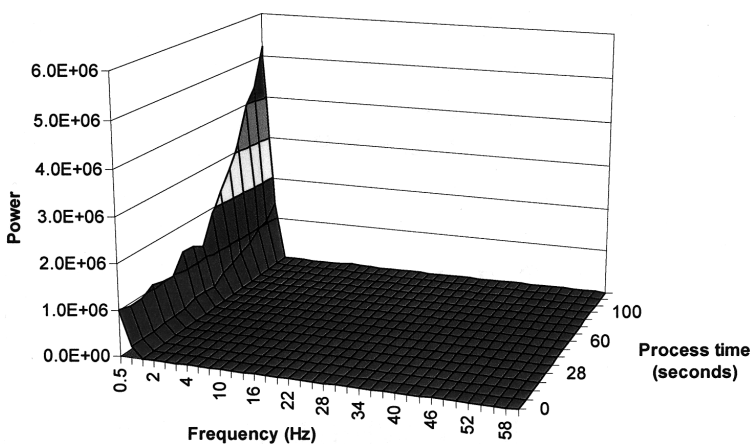


Fig. 8. Typical spectral data from 30-kHz sensor.

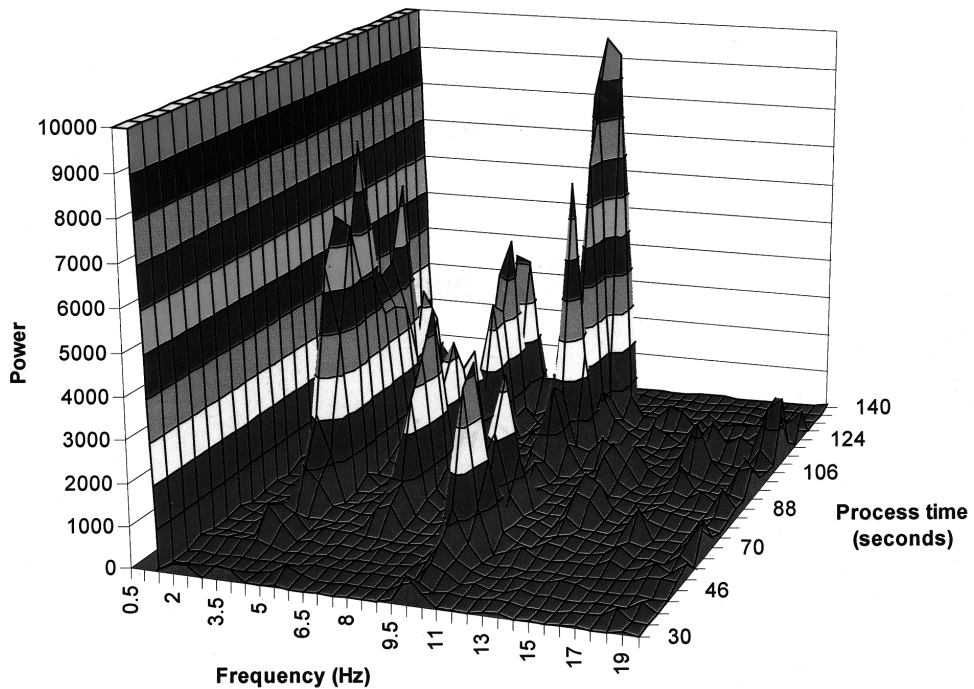


Fig. 9. Localized spectral peaks.

shown graphically for the 400-ml batch using the 30-kHz sensor in Fig. 8. The power spectrum shows peaks at localised frequency intervals of  $\sim 3.33$  Hz, reaching a local maximum at 10 Hz (Fig. 9). This reflects the speed of rotation of the mixer shaft at  $\sim 200$  rpm (3.33 Hz) in combination with the three mixer blades to give a local

maximum at 10 Hz. Therefore, acoustic spectral information could be used to measure accurately the speed of rotation of the mixer in real time. Signal frequency data were reviewed to determine which individual frequencies gave the best correlations using simple linear regression with particular physical parameters (i.e. which frequencies were

‘information rich’). Unlike most optical spectroscopic techniques (e.g. infra-red), it is not yet possible to predict which frequencies are likely to be present in the acoustic spectrum before starting a process monitoring experiment. Therefore, it is necessary to examine the spectral data obtained and compare this with a knowledge or measure of any changes in physical properties of the material being processed. Good univariate correlations (correlation coefficient ( $r$ ) greater than 0.95) could be obtained by selecting particular signal frequencies for simple linear regression with the physical data. However, this approach was found not to be robust from batch to batch. Correlations using a small number of discrete frequencies were also no better than those achieved using all frequencies.

In an attempt to overcome the problems of the univariate approach, multivariate calibration was investigated. However, given the small number of samples, the results should be considered merely as a guide to the existence of a relationship between the acoustic data and the physical properties of the granule. More data (batches) would be required to produce calibration models with greater predictive accuracy.

For each batch and each sensor, the spectral data recorded from the last 20 s of granulation were averaged before comparison with the physical properties (particle size, granule flow and compression properties) using partial least squares (PLS) multivariate regression analysis.

Ordinary least squares regression suffers from the problem of poor precision in estimating the model coefficients in circumstances where there is high correlation between the variables. Any future predictions based on such models are likely to be poor. The use of step-wise regression techniques under such circumstances will also not guarantee that important information may not be lost.

Partial least squares is a very useful and commonly applied technique in the area of multivariate analysis. It is useful for the treatment of data where typically it is likely that some, if not all, of the  $X$  variables are highly correlated, or where there are many more variables than objects. One example of such a situation is in the field of near infra-red spectroscopy, where a multivariate calibration is derived from a data set containing

absorption at many wavelengths on relatively few objects. The signal frequency data created from acoustic monitoring can be considered as an analogous situation.

Partial least squares was chosen as a more appropriate technique than principal component regression (PCR), in order to investigate the ability of the variables to act as predictors of a response. The weakness of PCR is that no information about the covariance of the variables to the response is used in the calculation of the principal components.

All data (acoustic and physical) were pre-processed by mean centring and then scaled to unit standard deviation before using a PLS2 algorithm (The Unscrambler, CAMO ASA, Norway). Due to the small data size, cross-validation of the models was not possible and, therefore, the number of significant PLS components was determined using leverage correction. For the purposes of comparison, the same number of PLS components was used for all calibration models.

To assess which sensor (and, therefore, which frequency range) provides the greater information on the physical properties of the granule, the PLS correlation coefficient (a measure of the linearity of the model) and the root mean squared error of prediction (RMSEP — a measure of the accuracy of the model) were compared. The results for the three sensors for both the mass median particle size and the Carr’s compressibility index are presented in Table 3.

The results show that calibration models for the 30-kHz sensor provide the best correlations and the lowest RMSEP. Consequently, the data from the 30-kHz sensor have been used in all of the subsequent analysis.

The particle size of a granule is known to affect tablet weight variation and granule flow. Therefore, data are presented in Table 4 which gives the PLS correlation coefficient and RMSEP obtained for the regression of the acoustic spectral data (30-kHz sensor) with the mass median particle size for granule before and after dry screening. A plot of the predicted mass median particle size against the actual (measured) value for the granule before dry screening is also presented in Fig. 10.

An adequate correlation and RMSEP were obtained for the material before dry screening. However, after dry screening, a poor correlation was obtained, with the resulting effect that the RMSEP (as a percentage of the range) increases.

A more direct measure of the granule flow properties is the Carr's compressibility index. Data are presented in Table 5 for the regression

of the 30-kHz acoustic spectral data with the measured Carr's compressibility index of granule at various stages in the process. A plot of the predicted Carr's compressibility index against the actual (measured) value for the granule before dry screening is also presented in Fig. 11. Good linear correlations and acceptable RMSEPs were obtained for the granule both before dry screening

Table 3  
Comparison of multivariate calibration models using different sensors

Acoustic sensor	Physical properties <sup>a</sup>	Correlation coefficient ( $r$ ) <sup>b</sup>	RMSEP <sup>b</sup>	Range <sup>c</sup>
30-kHz	Mass median particle size	0.906	203 $\mu\text{m}$	111–1492 $\mu\text{m}$
70-kHz		0.799	288 $\mu\text{m}$	
150-kHz		0.795	291 $\mu\text{m}$	
30-kHz	Carr's compressibility index	0.929	1.8%	12.7–29.8%
70-kHz		0.694	3.4%	
150-kHz		0.836	2.6%	

<sup>a</sup> Physical properties of granule before dry screening.

<sup>b</sup> All calibration models used two PLS components.

<sup>c</sup> Range of results obtained from nine batches.

Table 4  
Comparison of acoustic calibration models for the determination of mass median particle size of granule before and after dry screening

Stage of process	Range <sup>a</sup> , $\mu\text{m}$	Correlation coefficient, ( $r$ ) <sup>b</sup>	RMSEP <sup>b</sup>	
			$\mu\text{m}$	Percentage of range <sup>c</sup>
Before dry screen	111–1492	0.906	203	15
After dry screen	92.5–238	0.777	31.6	22

<sup>a</sup> Range of results obtained from nine batches.

<sup>b</sup> All calibration models used two PLS components.

<sup>c</sup> RMSEP as a percentage of the range of results obtained.

Table 5  
Comparison of acoustic calibration models for the determination of granule flow properties (Carr's compressibility index) at various stages in the manufacturing process

Stage of process	Range <sup>a</sup> , %	Correlation coefficient ( $r$ ) <sup>b</sup>	RMSEP <sup>b</sup>	
			%	Percentage of range <sup>c</sup>
Before dry screen	12.7–29.8	0.929	1.8	11
After dry screen	20.3–31.9	0.630	2.5	22
After dry screen and lubricated	15.9–23.0	0.916	0.8	11

<sup>a</sup> Range of results obtained from nine batches.

<sup>b</sup> All calibration models used two PLS components.

<sup>c</sup> RMSEP as a percentage of the range of results obtained.

Table 6  
Comparison of correlation models for compression properties

Range <sup>a</sup> , kg	Correlation coefficient ( <i>r</i> ) <sup>b</sup>	RMSEP <sup>b</sup>	
		kg	Percentage of range <sup>c</sup>
8.43–11.84	0.686	0.86	25

<sup>a</sup> Range of results obtained from nine batches.

<sup>b</sup> All calibration models used two PLS components.

<sup>c</sup> RMSEP as a percentage of the range of results obtained.

and after lubrication with magnesium stearate. As for the particle size calibration, a poor correlation (and consequently poor RMSEP) was obtained for the material after dry screening. Closer examination of the calibration plots showed that the Carr's compressibility index results for the lubricated material are not evenly distributed, with all but one of the results in the range 15.9–19.0. Therefore, the calibration model is highly influenced by one data point (150-ml batch). Removal of this one batch resulted in a correlation coefficient of only 0.669.

The exact cause of the poor correlations and accuracy of the calibration models for material after dry screening for both particle size and Carr's compressibility index has not been identified. It is highly probable that the 'normalisation' effect that occurs to the granule during the dry screening stage of the process is the principal factor. In terms of particle size, the process of dry screening reduces the mass median particle size of the over-granulated batches, but does not significantly change the under-granulated batches. Hence, the differences in acoustic spectra found during the granulation stage relate poorly to the physical properties of the processed granule.

In addition to the flow properties of a granule, the compression properties are also important. Therefore, the maximum crushing strength of tablets produced from each of the granules has been determined. Data are presented in Table 6 for the PLS coefficients and RMSEP for the regression of the 30-kHz acoustic spectral data with the maximum crushing strength of tablets. A

plot of the predicted maximum crushing strength against the actual (measured) value for the tablets is also presented in Fig. 12.

These results are similar to those obtained for the mass median particle size and Carr's compressibility index for the granule after the dry screening stage. However, it is clear from Fig. 12 that a relationship between the acoustic spectra of the granule in the high shear bowl and the maximum crushing strength of tablets exists.

Reasonable linear relationships have been found between the frequency spectrum of the acoustic signals and the physical properties of the granules before dry screening (mass median particle size and flow characteristics) and the tablets after compression (maximum crushing strength). However, after dry screening of the granule, the quality of the relationship significantly deteriorated. It has, therefore, not been possible to relate adequately the acoustic output from the granulator bowl to the final flow properties of the blend for compression. Consequently, this limited experimental study has been unable to demonstrate a clear correlation between the acoustic emissions produced during granulation and the tablet manufacturing properties. However, a strong correlation between acoustic emissions and the physical properties (particle size and flowability) of the granule at the end of the granulation process has been demonstrated. Thus, this procedure has clearly shown some potential as a granulation

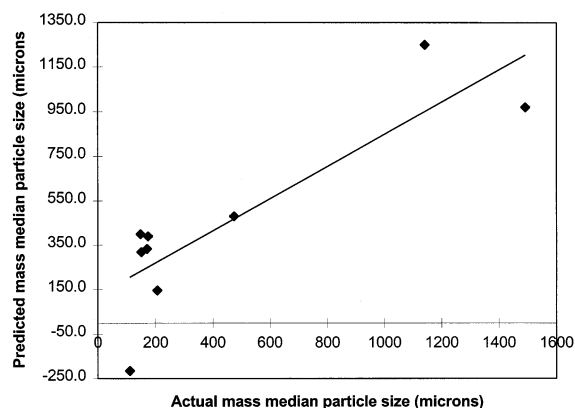


Fig. 10.

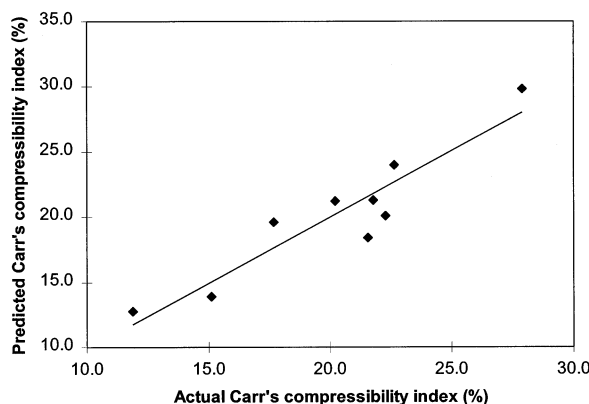


Fig. 11.

monitoring technique, although further work is required to establish whether it has the capability to monitor the properties of the final powder blend for tablet manufacture.

The technique could, therefore, be considered as a useful process analysis tool once further experimental studies are performed to understand better the full potential, as well as the inevitable limitations.

Acoustic monitoring has a number of advantages over the existing techniques used. In particular, it is non-invasive, inexpensive and has been shown to be sensitive. Experimental work performed on other pharmaceutical operations (unpublished work) has demonstrated that acoustic emissions can be used successfully to monitor these processes and that this technique, therefore, has a wider applicability than that presented in this paper.

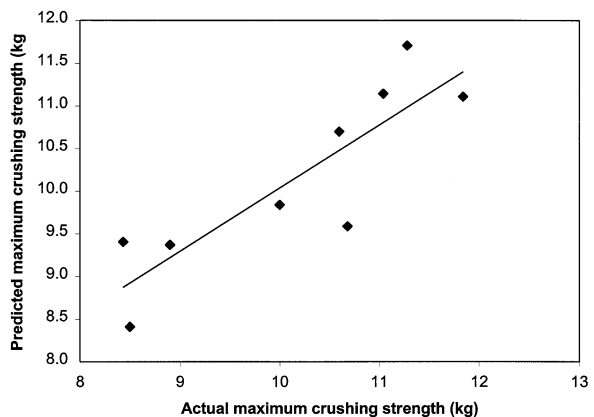


Fig. 12.

## References

Aulton, M.E., 1988. *Pharmaceutics: The Science of Dosage Form Design*. Churchill Livingstone, Edinburgh.

Belchamber, R.M., Betteridge, D., Collins, M.P., Lilley, T., Marczewski, C.Z., Wade, A.P., 1986. Quantitative study of acoustic emission from a model chemical process. *Anal. Chem.* 58, 1873–1877.

Betteridge, D., Joslin, M.T., Lilley, T., 1981. Acoustic emission of chemical reactions. *Anal. Chem.* 53, 1064–1073.

Holroyd, T.J., 1989. Acoustic emission from an industrial application viewpoint. *J. Acoust. Emiss.* 7, 193–199.

Tily, P.J., Porada, S., Scruby, C.B., Lidington, S., 1987. In: Harnby, N., Benkririra, H., Carpenter, K., Mann, R. (Eds.), *Proceedings of the Institution of Chemical Engineering Fluid Mixing III Symposium* (8–10 September). Hemisphere Publications Corporation, Madison Avenue, NY, pp. 75–94 Symposium Series No. 108.

van der Ziel, A., 1976. *Noise in Measurements*. Wiley, New York.

Wentzell, P.D. and Wade, A.P., 1989. Chemical acoustic emission analysis in the frequency domain. *Anal. Chem.* 61, 2638–2642.